JOURNAL OF VIROLOGY, Feb. 2007, p. 1610–1618 Vol. 81, No. 4
0022-538X/07/$08.00+0 doi:10.1128/JVI.01433-06

Heterogeneity of Raft-Type Membrane Microdomains Associated with VP4, the Rotavirus Spike Protein, in Caco-2 and MA 104 Cells▽

Olivier Delmas,[1] Michelyne Breton,[1] Catherine Sapin,[1] André Le Bivic,[2] Odile Colard,[1] and Germain Trugnan[1]*

INSERM UMRS 538, Faculty of Medicine Pierre et Marie Curie, site Saint Antoine, University Pierre and Marie Curie, 27 rue de Chaligny, 75012 Paris, France,[1] and NMDA, IBDM, Faculté des Sciences de Luminy, Case 907, 13288 Marseille, Cedex 09, France[2]

Received 7 July 2006/Accepted 17 November 2006

Previous studies have shown that rotavirus virions, a major cause of infantile diarrhea, assemble within small intestinal enterocytes and are released at the apical pole without significant cell lysis. In contrast, for the poorly differentiated kidney epithelial MA 104 cells, which have been used extensively to study rotavirus assembly, it has been shown that rotavirus is released by cell lysis. The subsequent discovery that rotavirus particles associate with raft-type membrane microdomains (RTM) in Caco-2 cells provided a simple explanation for rotavirus polarized targeting. However, the results presented here, together with those recently published by another group, demonstrate that rotavirus also associates with RTM in MA 104 cells, thus indicating that a simple interaction of rotavirus with rafts is not sufficient to explain its apical targeting in intestinal cells. In the present study, we explore the possibility that RTM may have distinct physicochemical properties that may account for the differences observed in the rotavirus cell cycle between MA 104 and Caco-2 cells. We show here that VP4 association with rafts is sensitive to cholesterol extraction by methyl-β-cyclodextrin treatment in MA 104 cells and insensitive in Caco-2 cells. Using the VP4 spike protein as bait, VP4-enriched raft subsets were immunopurified. They contained 10 to 15% of the lipids present in total raft membranes. We found that the nature and proportion of phospholipids and glycosphingolipids were different between the two cell lines. We propose that this raft heterogeneity may support the cell type dependency of virus assembly and release.

Rotavirus, a major cause of infantile diarrhea, is a nonenveloped virus that naturally infects small intestinal enterocytes. Using intestinal epithelial Caco-2 cells infected with rotavirus, our group demonstrated that virus particles were released in a nonlytic, highly polarized way to the apical poles of cells through an atypical trafficking pathway bypassing the Golgi apparatus (40). We then showed that raft-type membrane microdomains are involved in this atypical pathway and, more particularly, that VP4, the most peripheral protein of rotavirus, is rapidly associated with raft microdomains. The kinetics of virus protein arrival in rafts and the presence of virus infectivity (57) led us to propose that lipid rafts may serve as a platform for VP4 assembly with the rest of the particle. A role for lipid rafts during replication and transfer to the cell surfaces of Caco-2 cells was subsequently confirmed (18). Recent data also demonstrated that VP4 binds specifically to brush border actin bundles and remodels the bundles into actin bodies in Caco-2 cells (29). Together, these data support a role for rafts and actin in rotavirus final assembly and apical release in epithelial intestinal cells. Most former studies on rotavirus morphogenesis have been performed with MA 104 cells, a nondifferentiated kidney epithelial cell line. In this model, assembly of the third capsid layer (containing VP4) is thought to occur in the endoplasmic reticulum (ER), and mature viral particle release is associated with a concomitant lysis of infected cells (26, 46). However, with Caco-2 cells, we have shown that when rotavirus particles are blocked as enveloped particles in the ER, using tunicamycin, the targeting of VP4 to surface membranes and its association with raft membranes are not modified. This suggests that particle assembly with VP4 is an extrareticular event in the intestinal Caco-2 cell line (21). Very recently, using MA 104 cells, Cuadras et al. (17) showed that inhibition of rotavirus migration into lipid rafts, either by small interfering RNAs specific to VP4 and NSP4 or by tunicamycin, also specifically blocked the targeting of VP4 to rafts, suggesting that the association of VP4 with the particle takes place in the ER. Thus, the roles of raft membranes appear to be different in the enterocyte-like Caco-2 cell line and the renal MA 104 cell line. Therefore, we hypothesized that the raft membranes associated with VP4 could be different in MA 104 and Caco-2 cells and that the differences could account for the discrepancies observed between the two cell lines.

Since the initial description of rafts as an example of membrane heterogeneity (10), a huge number of works have been performed to try to delineate their compositions and functions. Biological membrane structure and dynamics rely on a large variety of lipids having different polar head groups, lengths, and unsaturation states of their fatty acid chains. Biophysical studies and high-resolution microscopy have revealed that these lipids do not form a homogeneous phase but, due to specific interactions between lipid species, organize within membrane microdomains with lateral segregation. In particular, the partitioning of cholesterol and sphingolipids, which

* Corresponding author. Mailing address: INSERM UMRS 538, Faculty of Medicine Pierre et Marie Curie, site Saint Antoine, University Pierre and Marie Curie, 27 rue de Chaligny, 75012 Paris, France. Phone: 33 1 4001 1340. Fax: 33 1 4001 1390. E-mail: trugnan@st-antoine.inserm.fr.

▽ Published ahead of print on 29 November 2006.

possess long saturated fatty acid chains, induces the formation of liquid-ordered phases (1, 8, 9, 19), creating patches called "rafts" separated from the rest of the membrane, which is in a liquid-disordered state. Based on the insolubility in detergents of membranes enriched in cholesterol, sphingolipids, and lipid-anchored proteins, such liquid-ordered phases were shown to exist in cell membranes as "detergent-resistant membranes" (DRM) (10; reviewed in reference 8). These liquid-ordered domains are thought to arise from the Golgi apparatus, where sphingolipids are synthesized (64) and to which they recruit proteins destined for apical trafficking in epithelial cells, as proposed by Simons and Ikonen as "the raft hypothesis" (60). These domains have also been implicated in cell signaling (61) and virus penetration, assembly, and release (14). A rapidly growing number of proteins have been shown to be "raft associated" (27). Depending on the method used, the size and nature of membrane rafts correspond to different entities, from relatively large structures (>50 nm) (52, 60, 65) to dynamic assemblies of small size (2) and to nanoscale organization (59). The coexistence of different raft populations was first suggested by the observation that various detergents solubilized membranes differently (58) and by distinct responses to cholesterol removal (43, 54). Cholesterol-independent "super-rafts" were also described for the intestinal brush border (34). Distinct raft populations were then identified through their function (31, 62) and/or lipid composition (12, 25).

We show here striking differences regarding the sensitivity to cholesterol extraction and the lipid composition of VP4-associated raft subsets in MA 104 and Caco-2 cell lines. Moreover, while VP4 is evenly distributed in the former cells, it is mostly present at the apical poles of the latter cells. We propose that the raft heterogeneity observed between the two cell lines may explain the cell type dependency of virus assembly and trafficking.

MATERIALS AND METHODS

Materials. (i) Detergents. Triton X-100 (TX-100), Brij 56, and NP-40 were purchased from Sigma-Aldrich (St. Louis, MO). Lubrol-WX was purchased from Serva (Heidelberg, Germany).

(ii) Antibodies. The anti-caveolin-1 (anti-Cav-1) rabbit polyclonal antibody N20, directed against N-terminal residues 2 to 21 of caveolin-1, was obtained from Santa Cruz Biotechnology (Santa Cruz, CA). Mouse monoclonal anti-Cav-1 (2234) and anti-flotillin-2/ESA (Reggie-1) antibodies were purchased from BD Transduction Laboratories (Lexington, KY). The anti-VP4 (7.7) mouse monoclonal antibody was a gift from J. Cohen (CNRS, Gif-sur-Yvette, France). M-450 Dynabeads were purchased from Dynal (New Hyde Park, NY). Goat anti-mouse immunoglobulin G (IgG) and anti-rabbit IgG conjugated to peroxidase were purchased from Sigma. The silica gel 60 high-performance thin-layer chromatography (HPTLC) plates used for lipid analysis were purchased from Merck (Darmstadt, Germany). A neutral glycosphingolipid mixture was obtained from Matreya, Inc. (Pleasant Gap, PA). The phospholipid standards (phosphatidylethanolamine, phosphatidylserine, phosphatidylcholine, and sphingomyelin) were purchased from Sigma-Aldrich.

Cell culture, labeling, infection, and immunofluorescence. MA 104 cells were cultured in Dulbecco's modified Eagle medium supplemented with 10% decomplemented fetal calf serum, 100 U/ml of penicillin, and 100 μg/ml of streptomycin and were passaged each week. Cells were grown in a 5% CO_2–air atmosphere at 37°C. For experiments, MA 104 cells were used between 5 and 6 days after plating. Caco-2 cells were cultured in Dulbecco's modified Eagle medium supplemented with 20% decomplemented fetal calf serum in the presence of 100 U/ml penicillin, 100 μg/ml streptomycin, and 1% nonessential amino acids. Cells were grown in a 10% CO_2–air atmosphere at 37°C. Caco-2 cells were used 15 days after reaching confluence (21 days of culture), and the medium was changed daily. Caco-2 cells were transfected with plasmids containing canine Cav-1 cDNA as previously described (7). Clones were used after overnight sodium butyrate (10 mM) induction. When cells were labeled with [^{3}H]cholesterol, 5 μCi per flask was added 18 h before the experiment for Caco-2 cells and Caco-2 cells expressing Cav-1 and just after plating for MA 104 cells. When cells were labeled with [^{14}C]serine, 5 μCi per flask was added just after plating for MA 104 cells, and 5 μCi per flask was added twice in the last 2 days before experiments with Caco-2 cells. Cells were infected with rotavirus strain RF, obtained from J. Cohen (CNRS, Gif-sur-Yvette, France), as previously described (57), at 10 PFU per cell for Caco-2 cells (transfected with Cav-1 or not) and at 3 PFU per cell for immunofluorescence and 1 PFU per cell for raft preparation when using MA 104 cells. For treatment with methyl-β-cyclodextrin (CD; Sigma), infected cells labeled with [^{3}H]cholesterol were incubated with 10 mM CD in infection medium for 1 h at 37°C, with gentle shaking. Where indicated, 10 μM lovastatin (Sigma-Aldrich) was added at 1 h postinfection (p.i.) and left until the end of the experiment. DRM were prepared just after the treatment. The efficiency of the CD treatment was monitored by counting [^{3}H]cholesterol in the culture medium and in DRM and soluble fractions obtained from treated and nontreated cells. Immunofluorescence and confocal microscopy analyses were performed on permeabilized cells grown on glass coverslips as previously described (57).

DRM preparation. Membranes resistant to TX-100 or other detergents at 4°C were prepared following flotation gradient separation as described previously (57). Briefly, cells were washed twice with phosphate-buffered saline, scraped into 2 ml TNE buffer (20 mM Tris-HCl, pH 7.4, 150 mM NaCl, 1 mM EDTA, and a cocktail of antiproteases [Complete Mini; Roche Diagnostics GmbH]) containing 1% TX-100 or other detergents, and passed 10 times through a 22-gauge needle. After 30 min at 4°C, the resulting homogenate was mixed with 2 ml 80% sucrose solution. Layers of 35 and 5% sucrose solution were added, and the discontinuous gradient was centrifuged at 180,000 × *g* for 18 h at 4°C in a Beckman SW 41 rotor. The DRM fraction was collected at the 5%-35% interface. Homogenates were sonicated with a microtip at a frequency of 20 kHz (MSE sonicator) twice for 10 s each before being analyzed as total membranes. When OptiPrep gradients were used, 1.34 ml of homogenate was mixed with 2.66 ml of pure OptiPrep (Sigma-Aldrich). Layers of 30% and 5% OptiPrep solution were added, and the discontinuous gradient was centrifuged at 100,000 × *g* for at least 4 h at 4°C in a Beckman SW 41 rotor. The DRM fraction was collected at the 5%-30% interface. Between 12 and 16 mg protein was used for sucrose gradients, and three times less was used for OptiPrep gradients.

Lipid extraction and analysis. Lipids from total membranes and from DRM were extracted with chloroform-methanol by phase separation as described by Bligh and Dyer (3). Phospholipids, cholesterol, and neutral glycosphingolipids were recovered from the lower chloroform phase. Solvents from the chloroform phase were evaporated under a stream of nitrogen, and the lipids were resuspended in chloroform-methanol (1/1 [vol/vol]). The total amount of phospholipids was determined for crude lipid extract by measurement of the phosphorus content (5). For sphingomyelin quantification, the main classes of phospholipids were separated on HPTLC plates by migration in chloroform-methanol-H_2O (65/25/4 [vol/vol/vol]) and were revealed by iodine vapor (13). Silica powder corresponding to sphingomyelin was scraped, and phosphorus content was determined on the powder. For cholesterol determination, an aliquot of lipid extract was evaporated and dissolved in ethanol, and the cholesterol content was determined by a colorimetric assay (28). To correctly separate the neutral glycolipids, it was necessary to eliminate the phospholipids by hydrolysis. Therefore, aliquots of lipid extracts were resuspended in 1 ml 0.5 N KOH-methanol and heated for 1 h at 56°C. After cooling, the lipids were separated according to the method of Bligh and Dyer (3). The chloroform phase was washed until neutralization and evaporated, and the neutral glycolipids were separated on HPTLC plates by migration in chloroform-methanol-H_2O (65/25/4 [vol/vol/vol]) and revealed by spraying with orcinol.

Western blot analysis and affinity purification of VP4-rich membrane complexes. Proteins recovered from the gradient fractions were separated by sodium dodecyl sulfate-polyacrylamide gel electrophoresis (SDS-PAGE) and electrotransferred to nitrocellulose sheets for immunoblotting as described previously (21). Protein assays were performed with a BCA kit (Pierce, Rockford, IL). To isolate VP4-associated membrane complexes, VP4 was immunoprecipitated from DRM fractions prepared from [^{3}H]cholesterol-labeled or [^{14}C]serine-labeled infected cells, using magnetic beads. In order to maintain raft integrity, the DRM fraction obtained after sucrose gradient separation was gently resuspended in gradient medium by passage through a 22-gauge needle as described for DRM preparation, with all procedures carried out at 4°C. Magnetic separation also contributes to conserving membrane integrity by eliminating all centrifugation steps. M-450 Dynal beads conjugated with anti-mouse IgG were washed three times with TBS-BSA (20 mM Tris-HCl, pH 7.5, 140 mM NaCl, 0.2% bovine serum albumin) by resuspension and magnetic separation. The

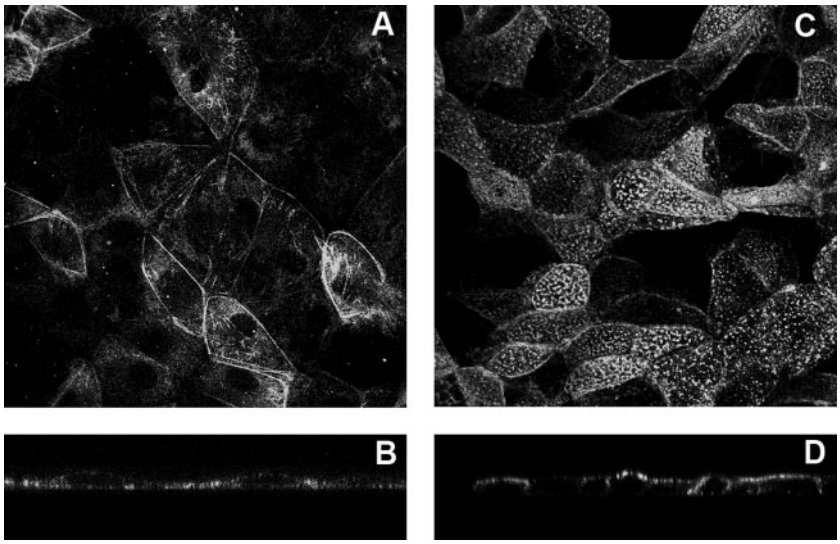

FIG. 1. VP4 mostly localizes at the apical membranes of Caco-2 cells, whereas no particular localization was observed in MA 104 cells. MA 104 cells (5 days old) and Caco-2 cells (20 days old) were infected with the RF rotavirus strain at 3 PFU/cell and 10 PFU/cell, respectively. VP4 was detected after cell permeabilization, using monoclonal antibody 7.7 and a fluorescein isothiocyanate-labeled secondary anti-mouse IgG antibody, and observed by confocal microscopy as described in Materials and Methods. (A and B) MA 104 cells. (C and D) Caco-2 cells. (A and C) *xy* projections. (B and D) *xz* sections.

anti-VP4 monoclonal antibody was then bound to washed beads by overnight incubation (2×10^7 beads and 4 μg IgG) on a rotary shaker. After being washed three times with TBS and one time with TNE and 1% TX-100, the anti-VP4 beads were resuspended in TNE–1% TX-100. DRM fractions (10 μg of proteins) were precleared by incubation with washed beads for 2 to 3 h and then incubated with anti-VP4-associated beads for 3 to 4 h, with gentle shaking. Magnetic separation allowed us to isolate bound and unbound material. The entire procedure was performed at between 4 and 8°C. The beads were then washed with TNE–1% TX-100 three times, resuspended in Laemmli buffer (2% SDS, 10% glycerol, 60 mM Tris, pH 6.8, 2% β-mercaptoethanol), and heated at 100°C for 5 min. Radioactivities present in bound and unbound material and in starting DRM were counted in a Beckman liquid scintillation spectrometer after the addition of Ultima Gold (Perkin-Elmer) scintillation fluid. Total DRM and VP4-associated membrane complexes were subjected to SDS-PAGE and Western blot analysis. Conditions for caveolin and flotillin immunoprecipitation were 3×10^7 beads and 5 μg IgG with the 2234 monoclonal anti-Cav-1 antibody and 2×10^7 beads and 2 μg IgG with the anti-flotillin-2/ESA antibody. [^{14}C]serine-labeled lipids obtained after immunoseparation were extracted and separated on HPTLC plates. The radioactivity was detected and quantified using a phosphorimager (Storm 860; Amersham Pharmacia Biotech) and ImageQuant software.

RESULTS

The rotavirus VP4 spike protein localizes differently in MA 104 and Caco-2 cells. Using indirect immunofluorescence and confocal microscopy, VP4 has been shown to be present at the plasma membranes of MA 104 cells infected with the rotavirus strain RF (48). It was estimated that VP4 plasma membrane fluorescence represented around 20% of the total signal. Using Caco-2 cells, we previously observed that early after rotavirus infection, VP4 was specifically expressed at the apical membrane, where it resisted a short treatment by Triton X-100 at 4°C (57). The enterocyte-like Caco-2 cells, used to study rotavirus cell tropism and polarized release, are tight and thick when they are infected 21 days after being plated. The viral particles start to be released from these cells at 20 h p.i. (40). The flat epithelial renal MA 104 cells have classically been used to multiply the virus, and viral particles start to be released after 6 h p.i. through cell lysis (26, 46). Here we compared VP4 localization in infected MA 104 and Caco-2 cells at comparable times with regard to progeny virion assembly, i.e., at 2 h p.i. for MA 104 cells and 6 h p.i. for Caco-2 cells, that correspond to the times at which VP4 started to be detectable by Western blotting. Using the monoclonal antibody 7.7 to visualize VP4, very different patterns were observed between the two cell lines. The punctate staining of Caco-2 cells (Fig. 1C) is typical of brush border labeling, whereas in MA 104 cells a more diffuse labeling was observed (Fig. 1A). *xz* sections confirmed that VP4 staining was almost exclusively present at the level of the brush borders of highly differentiated Caco-2 cells (Fig. 1D), whereas VP4 was mainly present within the cytoplasm of MA 104 cells and was seen faintly at the membrane (Fig. 1B). These observations are in good agreement with recent work from our lab (29) that demonstrated that VP4 strongly associated with the actin cytoskeleton and, more precisely, with actin bundles that specifically localize at the apical brush border in intestinal Caco-2 cells, thus explaining the punctate staining, which does not exist in nondifferentiated MA 104 cells.

Membrane cholesterol removal differently affects VP4 association with rafts in the two cell lines. Previous work has shown that VP4 associates with DRM during virus penetration in MA 104 cells (37) and that infection is sensitive to cholesterol extraction by CD (33, 56), supporting the possibility that rafts may be implicated in rotavirus penetration. Whether neosynthesized VP4 may associate with rafts in MA 104 cells during virus assembly was not known until recently. Cuadras et al. recently showed the presence of viral proteins within rafts in MA 104 cells at 9 h p.i. (17). We also show here, using immunoblotting, that VP4 associates with rafts of MA 104 cells at 6 h p.i., as shown in Fig. 2A. The proportion of VP4 that associated with rafts in this cell line was not significantly different from the amount of VP4 recovered in the raft fraction of Caco-2 cells at a comparable time with regard to progeny

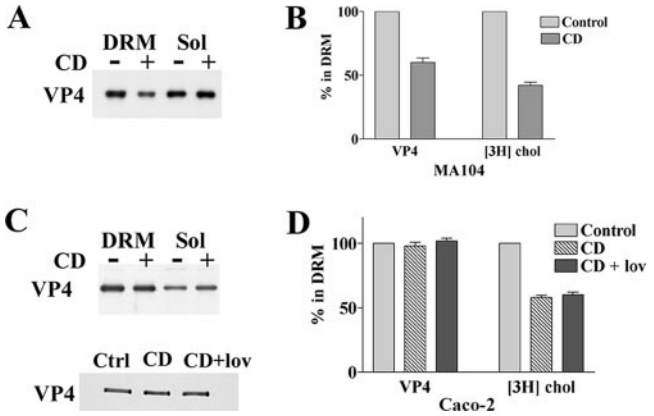

FIG. 2. VP4 association with DRM is sensitive to methyl-β-cyclodextrin treatment in MA 104 cells and insensitive in Caco-2 cells. MA-104 (A and B) and Caco-2 (C and D) cells were cultured, labeled with [^{3}H]cholesterol, and infected with rotavirus as described in Materials and Methods. CD was added to cells at 6 h and 18 h postinfection for MA 104 and Caco-2 cells, respectively. Where indicated, lovastatin (lov) was added at the beginning of the postinfection time. After OptiPrep gradient separation of lysed cells, the floating material (DRM) and the soluble fractions (the bottom four 1-ml fractions [Sol]) were collected and analyzed for VP4 content. Blots were quantified using Scion image software. [^{3}H]cholesterol contents were determined by radioactivity counting. VP4 and cholesterol contents were expressed as percentages of DRM related to control cells ($n = 4$ and 6 for MA 104 and Caco-2 cells, respectively).

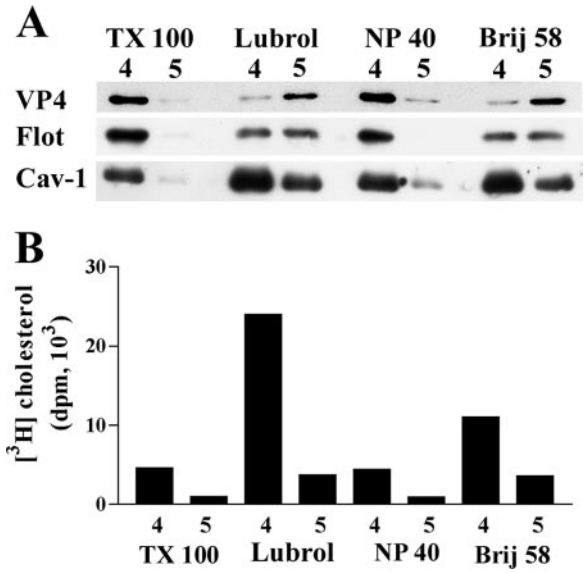

FIG. 3. VP4 and caveolin expression in DRM from MA 104 cells. MA 104 cells were infected and labeled with [^{3}H]cholesterol as described in the legend to Fig. 2. Cells were then lysed in TNE buffer containing 1% of one of the following detergents: TX-100, Lubrol-WX (Lubrol), Nonidet P-40 (NP-40), or Brij 58. After flotation on a sucrose gradient, 1-ml fractions were collected from the top. (A) Fractions 4 and 5, corresponding to floating material, were analyzed by SDS-PAGE and Western blotting for the virus protein VP4, flotillin (Flot), and caveolin-1 (Cav-1). (B) Radioactivities in fractions were counted, and cholesterol content is expressed as disintegrations per minute (dpm) for individual fractions.

virion assembly, i.e., at 18 h p.i. (VP4 present in DRM was 43% ± 6% [$n = 4$] and 38% ± 7% [$n = 8$] for MA 104 and Caco-2 cells, respectively).

Sensitivity to cholesterol extraction has long been considered a major criterion for protein association with rafts (41). We therefore examined the sensitivity to cholesterol extraction of VP4 associations with rafts in the two cell lines. [^{3}H]cholesterol-labeled steady-state MA 104 or Caco-2 cells were treated or not treated with the cholesterol-extracting drug CD, and DRM were subsequently prepared. Radioactivity was then counted in soluble and DRM fractions. As shown in Fig. 2A, incubation of MA 104 cells with 10 mM CD for 1 hour at 6 h p.i. decreased the amount of VP4 associated with DRM by 40%, while 60% of cholesterol was extracted (Fig. 2B). VP4 was essentially extracted in the medium, since it was not quantifiably recovered in the soluble fraction. This is consistent with recent data showing that CD also extracts large amounts of phospholipids and decreases the amount of glycosylphosphatidylinositol (GPI)-linked receptors (36, 55). In contrast, a similar incubation, at 18 h p.i., of Caco-2 cells with CD had no significant effect on the association of VP4 with DRM (Fig. 2C). The addition of 10 μM lovastatin, a drug that blocks cholesterol synthesis, had no further effect (Fig. 2C). In this cell line, cholesterol extraction (Fig. 2D), with or without lovastatin, was lower than that in MA 104 cells (42% ± 3% [$n = 4$]). Treatment of Caco-2 cells with 30 mM CD increased cholesterol extraction up to 50%, with still no detectable effect on VP4 DRM association (data not shown).

Caveolin expression status does not explain the different sensitivities of MA 104 and Caco-2 cells to CD. A striking particularity of Caco-2 cells, as well as of normal intestinal cells, is the absence of Cav-1 expression (45). We used two complementary approaches to investigate whether or not the absence of caveolin could account for the differences in VP4 association with DRM in MA 104 and Caco-2 cells. First, different detergents were tested for the ability to resolve VP4-containing DRM from caveolin-containing DRM in MA 104 cells. Detergent extracts were analyzed on sucrose gradients, and most of the floating material was recovered within two fractions (fractions 4 and 5). As expected from previous data (54, 58), detergent extractions resulted in very different patterns. TX-100 and NP-40 extracted most of the DRM-associated VP4, Cav-1, and flotillin within fraction 4 (Fig. 3A), as well as cholesterol-associated DRM (Fig. 3B). In contrast, Lubrol WX and Brij 58 behaved differently, since VP4 was mostly recovered in fraction 5 and flotillin was equally present in the two fractions, whereas Cav-1 was predominantly recovered in fraction 4 (Fig. 3A), as was DRM-associated cholesterol (Fig. 3B). These results indicate that when detergents are allowed to separate the DRM content into two fractions (i.e., using Lubrol WX or Brij 58), the distributions of VP4 and Cav-1 do not match. It is interesting that the DRM fractions from Lubrol WX and Brij 58 extractions were much more enriched in cholesterol than were TX-100- and NP-40-extracted DRM.

In a second set of experiments, Caco-2 cells were stably transfected with Cav-1, and the effects of CD on VP4 association with DRM were compared in Cav-1-transfected and wild-type Caco-2 cells. Analysis of Cav-1 distribution in a sucrose gradient of TX-100-extracted cells (Fig. 4A) confirmed that Cav-1 was concentrated within DRM fraction 4 of Caco-2

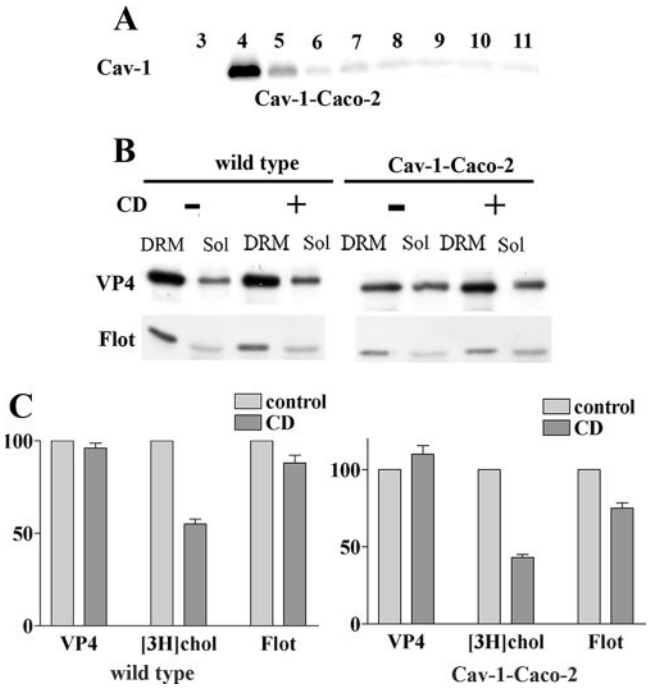

FIG. 4. Cell type-dependent sensitivity of VP4 association with DRM to cholesterol extraction does not depend on caveolin expression. (A) Caco-2 cells stably transfected with caveolin-1 (Cav-1-Caco-2) were cultured for 10 days after reaching confluence. Transfected caveolin-1 distribution along a sucrose gradient after cell lysis in TX-100 at 4°C is shown. Note that wild-type Caco-2 cells do not express any detectable Cav-1 (not shown). (B) Cav-1-expressing and wild-type Caco-2 cells were radiolabeled with cholesterol and infected with rotavirus (10 PFU/cell). They were not treated or treated with 10 mM CD before cell lysis, gradient separation, and DRM collection. Equal amounts (in volume) of floating materials (DRM) and soluble fractions (Sol) were collected and analyzed for VP4 and flotillin (Flot) content by SDS-PAGE. (C) [^{3}H]cholesterol, VP4, and flotillin were quantified and expressed as described in the legend to Fig. 2. Data are the means ± standard deviations for two different experiments. Gray bars, untreated cells; black bars, CD-treated cells.

cells. Wild-type and Cav-1-transfected Caco-2 cells were labeled with [^{3}H]cholesterol and infected with rotavirus. The level of VP4 expression was slightly lower in Cav-1-expressing than in wild-type Caco-2 cells. Cells were treated or not with 10 mM CD, and DRM fractions were prepared using TX-100. It should be noted that, as already demonstrated for other cell lines, CD was unable to extract Cav-1 from DRM of Cav-1-expressing Caco-2 cells (35; data not shown). Figure 4B and C show that VP4 was still associated with DRM in the presence of the drug in Cav-1-expressing as well as wild-type Caco-2 cells. It is interesting that Cav-1 expression restored cholesterol extractability (compare Fig. 4C with Fig. 2B). In spite of this fact, Cav-1 expression did not allow the dissociation of VP4 from DRM by CD. From these results, it can be concluded that VP4 association with DRM does not depend on caveolin expression in either MA 104 or Caco-2 cells.

VP4 association with DRM does not depend on their gross lipid composition. The above results indicated that the same protein, namely, VP4, associated differently with DRM from two distinct cell types in a manner that does not depend on caveolin content or on the extent of cholesterol extraction by

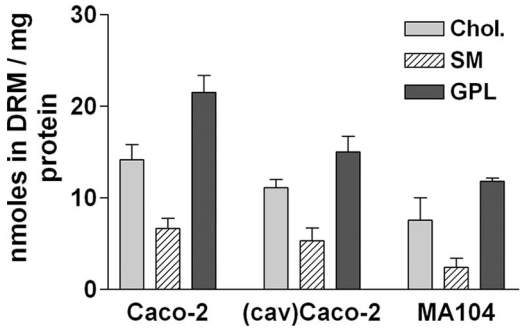

FIG. 5. DRM in the two cell lines essentially differ by the total amount of lipids. DRM were collected from MA 104 cells and from Cav-1-transfected and wild-type Caco-2 cells and were analyzed for cholesterol (Chol.), sphingomyelin (SM), and glycerophospholipid (GPL) contents as described in Materials and Methods. Data are expressed in nmol of lipids recovered in DRM per mg of cell protein initially layered on the gradient and are means ($n = 6$ for Caco-2 cells, $n = 3$ for MA 104 cells, and $n = 2$ for Cav-1-expressing Caco-2 cells).

CD. To find out the mechanism by which VP4 could differentially associate with DRM from different cell types, studies of the lipid compositions of these different DRM were undertaken. In a first set of experiments, the three major components of DRM, namely, cholesterol, sphingomyelin, and glycerophospholipids, were analyzed in MA 104 and Caco-2 cells. The ratios between glycerophospholipids and cholesterol were not significantly different ($P > 0.05$ in the nonparametric Mann-Whitney test) between the cell lines (Fig. 5). However, the ratio between cholesterol and sphingomyelin appeared to be different ($P < 0.05$), with the amount of sphingomyelin being somewhat lower in MA 104 than in Caco-2 cells. This fact shows that slightly different membrane microdomains may be selected by the same detergent, namely, TX-100, in different cell types. Moreover, it was observed that the total amount of lipid species present in the DRM fractions relative to the amount of proteins was about two times higher in differentiated Caco-2 cells than in undifferentiated MA 104 cells. The lipid content of DRM from transfected Cav-1-expressing Caco-2 cells was intermediate between those of DRM from Caco-2 and MA 104 cells.

Glycolipid analysis of MA 104 and Caco-2 cells reveals huge differences. Besides cholesterol and sphingomyelin, glycosphingolipids are also important components of raft-type microdomains. These compounds, which are relatively minor components of cell membranes, are concentrated in the TX-100 insoluble fraction (10). To study the glycolipid compositions of MA 104 and Caco-2 cells, lipids were extracted from total homogenates and separated by TLC. Phospholipids were observed following coloration with iodine. Glycolipids were observed following coloration with orcinol after phospholipid hydrolysis. The patterns of phospholipids were comparable (not shown), but the profiles of neutral glycolipids present in the two cell lines were different (Fig. 6). The two cell lines contained mostly monohexosides (also named cerebrosides), but Caco-2 cells contained more di- and trihexosides (also named lactosyl-ceramide and globoside-3, respectively) than did MA 104 cells. The glycolipids also differed in the fatty acid chain esterifying the ceramide moieties of glycolipids. This chain can be hydroxylated twice, and in that case, neutral

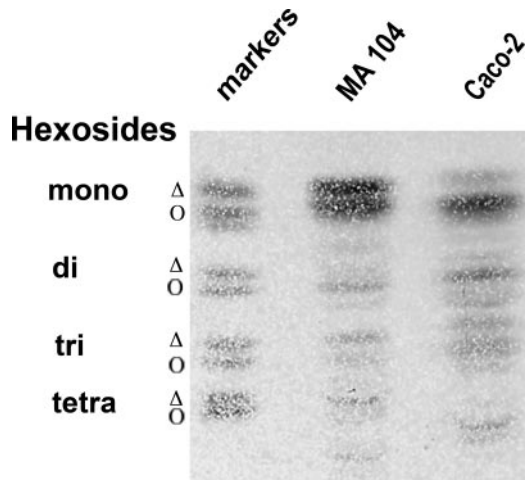

FIG. 6. Profiles of glycolipids from Caco-2 and MA 104 cells are highly different. Cells were scraped into TNE buffer and sonicated, and glycolipids were extracted as described in Materials and Methods. Glycolipid amounts corresponding to 1 mg protein in MA 104 and Caco-2 cell homogenates were spotted onto silica HPTLC plates. Migration was performed in chloroform-methanol-H_2O (65/25/4 [vol/vol/vol]). The plate was sprayed with orcinol for glycolipid visualization. Glycolipid markers were mono (or cerebrosides)-, di (or lactosyl-ceramides)-, tri (or globoside 3)-, and tetra (or globoside 4)-hexosides. For mono-, di-, and trihexosides, two main bands were revealed that corresponded to the nonhydroxylated (Δ) and hydroxylated (O) forms of the fatty acid chain esterifying the ceramide moiety.

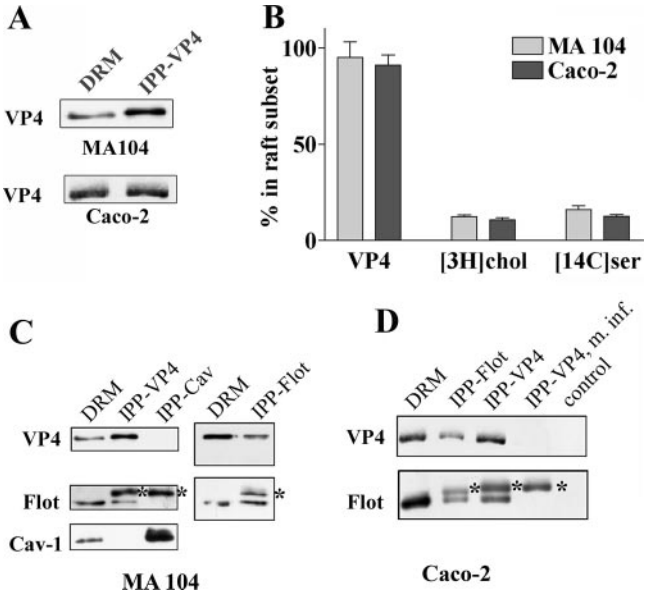

FIG. 7. Isolation of VP4-associated DRM subsets from both cell lines. DRM collected from MA 104 or Caco-2 cells, unlabeled or labeled with [^{3}H]cholesterol or [^{14}C]serine, were gently dissociated by passage through a 22-gauge needle. DRM suspensions were then incubated with anti-VP4 antibody bound to magnetic beads as described in Materials and Methods. After being washed, the beads were directly counted for [^{3}H]cholesterol or treated with chloroform-methanol for lipid extraction. A fraction of the beads was resuspended in Laemmli buffer and analyzed by Western blotting for VP4 content. (A) Typical VP4 recovery after immunoprecipitation. Double amounts for MA 104 cells and equal amounts for Caco-2 cells of immunoprecipitated fractions (IPP-VP4) related to DRM were spotted. (B) Percent recovery (related to total amount present in DRM) of VP4 and [^{3}H]cholesterol ([^{3}H]chol)- and [^{14}C]serine ([^{14}C]ser)-labeled lipids in the fraction immunoprecipitated with anti-VP4 antibody. VP4 ($n = 6$) was determined by densitometry, [^{3}H]cholesterol ($n = 6$) was directly counted on immunoprecipitated beads, and [^{14}C]serine ($n = 3$) was counted in the lipid extract. (C and D) DRM from MA 104 and Caco-2 cells were immunoprecipitated either with anti-VP4 antibody as in panel A or with anti-flotillin-2 or anti-caveolin-1 (2297) monoclonal antibodies. Fractions immunoprecipitated with anti-VP4 (IPP-VP4), anti-flotillin-2 (IPP-Flot), or anti-caveolin-1 (IPP-Cav) antibodies and a fraction of initial DRM were analyzed by Western blotting with anti-VP4, anti-flotillin-2, and anti-caveolin-1 (N-20) antibodies. m. inf., mock-infected cells; control, infected cells immunoprecipitated without antibody. Asterisks indicate immunoglobulin heavy chain spots.

glycolipids are more retained than their parent compounds in the chromatographic separation. As shown in Fig. 6, monohexosides are mostly dihydroxylated in Caco-2 cells and equally mono- and dihydroxylated in MA 104 cells. This result, together with the smaller amount of sphingomyelin, provided the first evidence that the global compositions of raft-type microdomains from MA 104 and Caco-2 cells are qualitatively different.

Isolation of subsets of VP4-rich membrane complexes from DRM fractions in MA 104 and Caco-2 cells reveals significant differences in lipid composition. To further explore potential differences between the two cell lines, the lipids associated with VP4 were directly studied in more detail, using an immunoprecipitation method that should preserve the integrity of DRM domains. Immunoprecipitation experiments were carried out on DRM prepared by sucrose gradient centrifugation from infected cells that were radiolabeled either with [^{3}H]cholesterol or with [^{14}C]serine. It is well established that serine is incorporated during the first step of ceramide synthesis (63) and then radiolabels sphingomyelin and glycosphingolipids. It also labels phosphatidylserine and phosphatidylethanolamine but not phosphatidylcholine (63). The recovery of VP4 from DRM from the two cell lines was almost complete, using the 7.7 monoclonal anti-VP4 antibody bound to magnetic beads (Fig. 7A and B), whereas around 12% of [^{3}H]cholesterol and 14% of [^{14}C]serine were present in the lipid extracts prepared from immunoprecipitated beads of both cell lines (Fig. 7B). Identical immunoprecipitations were carried out with mock-infected cells or with infected cells and magnetic beads without antibody (control) as negative controls (Fig. 7D). In these controls, no VP4 and $<1\%$ of radioactive lipids were immunoprecipitated, indicating that the immunoprecipitation was specific and leading us to isolate VP4-associated lipid raft domains (VP4-rafts). The scaffolding protein flotillin, expressed in raft-type membranes of different cell lines (66), was shown to strongly associate with VP4-selected DRM subsets in both cell lines, since reciprocal coimmunoprecipitation was regularly observed (Fig. 7C and D). In contrast, it was interesting that Cav-1, which is expressed only in DRM from MA 104 cells, did not coimmunoprecipitate with VP4 or with flotillin, confirming that Cav-1 was not involved in the VP4-DRM association.

[^{14}C]serine-labeled lipids were analyzed using TLC and autoradiography, and the DRM overall lipid composition was compared to the composition of DRM subsets isolated after specific VP4 immunoprecipitation. In MA 104 cells, the amount of sphingomyelin increased, whereas phosphatidyleth-

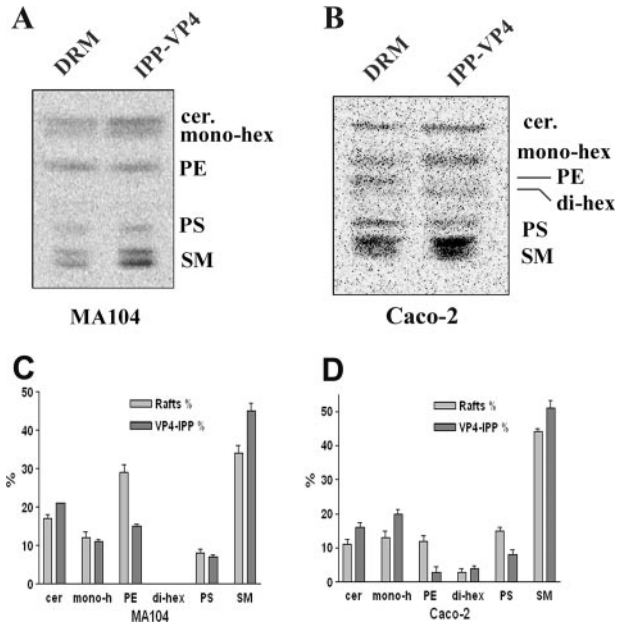

FIG. 8. Cell type differences in the lipid compositions of VP4-associated DRM subsets isolated from MA 104 and Caco-2 cells. (A and B) Typical separations by HPTLC of lipid extracts from [^{14}C]serine-labeled MA 104 (A) and Caco-2 (B) cells. Lipids from DRM and immunoprecipitated (IPP) fractions, as described in the legend to Fig. 7, were extracted and separated by HPTLC as described in the legend to Fig. 6. Radioactivity was detected by phosphorimager screening. Migration of lipid standards is indicated. Cer, ceramide; hex, hexoside; PS, phosphatidylserine; PE, phosphatidylethanolamine; SM, sphingomyelin. (C and D) Quantification of the data in panels A and B was performed using ImageQuant software. Data are expressed as the percentage of each lipid species, considering 100% to be the sum of all species in each sample ($n = 3$).

anolamine decreased in the VP4-immunoprecipitated subsets related to initial DRM (Fig. 8A and C). Ceramides, monohexosides, and phosphatidylserine were not significantly modified. Due to their higher content of glycolipids (Fig. 6), more radiolabeled spots were observed in Caco-2 cells (Fig. 8B). In this cell line, VP4-associated DRM subsets were also enriched in sphingomyelin and contained less phosphatidylethanolamine and phosphatidylserine. Interestingly, the amount of monohexosides increased in VP4-associated DRM subsets prepared from Caco-2 cells. Quantification of labeled spots (Fig. 8C and D) confirmed that VP4-associated DRM subsets were enriched in glycolipids only in Caco-2 cells. From these data, it can be concluded (i) that total DRM from the two cell lines have distinct lipid compositions and (ii) that VP4 is associated with DRM subsets whose lipid compositions are different from that of the total DRM population and which are different in the two cell lines, especially with regard to their neutral glycolipid content.

DISCUSSION

We previously attributed the fact that rotavirus was released, without any lysis, at the apical poles of polarized Caco-2 cells to the association of the rotavirus VP4 spike protein with raft-type membrane microdomains (57). However, although rotavirus is released by cell lysis in MA 104 cells, we and others (17) demonstrated that VP4 also associates with raft membranes in this cell line. To try to understand the molecular basis of this difference (lysis versus nonlysis) in the two cell lines, we therefore hypothesized that VP4 may associate with different raft subsets in the two cell lines and that this raft heterogeneity may explain the observed differences in the virus cell cycle. Our results show that VP4-associated raft-type membrane microdomains are effectively different in the two cell lines: VP4 association with rafts is sensitive to CD treatment in MA 104 cells and insensitive in Caco-2 cells, and the lipid compositions of VP4-associated raft subsets differ between the two cell lines, especially with regard to the amount and nature of hexosylceramides and the extent of acyl chain hydroxylation.

It is already known that raft heterogeneity exists and may support distinct functions. The group of Hakomori was the first to separate by immunoisolation a GM3 ganglioside enriched from a caveolin-containing fraction in the low-density TX-100 insoluble fraction of B16 melanoma cells (38). Different detergents were also used to demonstrate raft heterogeneity in MDCK cells: prominin associated with Lubrol-WX DRM, whereas alkaline phosphatase associated with both TX-100 and Lubrol-WX DRM (54). Two raft populations, operating in direct and transcytotic apical trafficking, respectively, were also identified in HepG2 hepatic cells on the basis of their resistance to extraction by different detergents (62). Surprisingly, despite the description of different raft subsets on the basis of their differential protein content, there are only a few studies on the lipid compositions of particular raft subsets. Brugger et al. recently observed that raft subsets immunoprecipitated with Thy-1 were enriched in hexosylceramides and contained more unsaturated and longer lipid chains than did prion protein-associated raft subsets (12). The present results reinforce the idea that raft heterogeneity is supported by distinct lipid compositions. Indeed, we show with two distinct cell lines that it is possible to immunoisolate a subset of raft-type microdomains, using VP4 as bait, whose lipid composition differs from that of the global population of raft microdomains. Even more, comparison of both the global populations of raft microdomains and VP4 raft subsets between the two cell lines indicates that they are also different.

First, we show that the nature of the glycolipids involved in raft formation is distinct in the two cell lines. The overall population of rafts from MA 104 cells is mainly composed of monohexosides and nonhydroxylated fatty acid chains, in contrast to the case for Caco-2 cells. These data point to a simple idea, that cells assemble lipid species synthesized through the metabolic pathways available in a given cell line into raft-type membrane microdomains on the basis of lipid-lipid specific interactions. Recruitment of specific lipids will then confer unique physicochemical properties to these microdomains. A clear example is given by recent observations that intestinal cells produce particular rafts, termed "super-rafts," assembled as highly stable and large entities resistant to cholesterol extraction (34). Our finding that Caco-2 rafts contain more different neutral glycolipids with more hydroxylated chains strongly argues for a reinforcement of lateral interactions within the plane of membrane lipids due to an increased number of hydrogen bond-accepting capacities (4, 39, 51; reviewed in references 11 and 44). This also may explain why cholesterol removal may be of little importance for the functionality of

rafts from Caco-2 cells, due to the above-mentioned hydrogen bonding between the head groups of glycolipids and/or to a lesser accessibility of cyclodextrin to cholesterol entrapped in these rafts (50, 53). We think that these physicochemical properties of Caco-2 raft-type microdomains are sufficient to explain why VP4 remains associated with these microdomains in the presence of CD.

Second, we show that the rotavirus VP4 spike protein binds to different raft subsets in MA 104 and Caco-2 cells. It is important that the immunoprecipitation approach used in the present study is rather efficient, since >90% of VP4 present in the total raft population was recovered within the VP4-associated raft subsets of both cell lines, together with 10 to 15% of total cholesterol and serine-labeled lipids. This indicates that quantitative information may be derived from our data. Since the general populations of raft-type microdomains from MA 104 and Caco-2 cells are different, it is not surprising to find that VP4 binds to different raft subsets. Our results indicate that this is the case and therefore support the idea that VP4 selects lipids within the total raft population on the basis of both affinities and the availability of particular lipid species. However, the enrichments in lipid species within the raft subsets relative to the initial raft populations were not the same in the two cell lines. VP4-associated raft subsets from MA 104 cells were mostly enriched in sphingomyelin and contained less phosphatidylethanolamine, whereas subsets from Caco-2 cells were enriched in both sphingomyelin and glycolipids and contained less phosphatidylethanolamine and phosphatidylserine. The mechanisms for such differences are not known, but it can be hypothesized that they might be due to the affinities of VP4 for different membrane lipids.

At least four domains have been identified in the sequence of VP4 that may mediate its interaction with membrane lipids. VP4 contains a fusogenic domain (42) which is able to permeabilize liposomes (23), a raft-independent membrane binding domain (30), an integrin binding domain thought to mediate virus attachment and/or entry into target cells (32), and a galectin-like domain within the N-terminal part of the protein that is thought to be located at the most external part of the virus spike (24). The fusogenic domain of VP4 was shown to interact with phosphatidylcholine- and cholesterol-containing liposomes in the absence of glycolipids (47). The integrin binding domain was shown to contain a GDE(A) sequence responsible for interaction with $\alpha 2\beta 1$ integrin in several cell lines from different origins (15). As a consequence, the first three domains do not seem to be involved in cell type-dependent differential interactions of VP4 with raft-type membrane microdomains. We suggest that the galectin-like domain of VP4 may be responsible for the preferential binding of VP4 with rafts in Caco-2 cells. This hypothesis fits very well with the observation that an authentic galectin, namely, galectin-4, a β-galactoside-specific lectin, interacts with intestinal raft-type microdomains (20) and that this interaction is CD insensitive (34), as shown here for VP4, dependent on glycolipids (6, 22), and directly involved in an apical targeting pathway (20). Indeed, a small interfering RNA specific for galectin-4 was recently shown to block apical trafficking in enterocyte-like cells (20). In 1990, a novel secretory mechanism was described for members of the galectin protein family which are abundant in the extracellular matrix (16). Galectins were shown to follow the "nonclassical secretory pathway," by-passing the Golgi apparatus, and to be secreted into the extracellular medium (49). It is tempting to speculate that rotaviruses follow the same intestinal raft-type microdomains as galectin-4 to reach the apical plasma membranes of Caco-2 cells. Further experiments are in progress to study the precise relationships between galectins and VP4 apical trafficking in Caco-2 cells.

ACKNOWLEDGMENTS

This work is dedicated to Jean Cohen, who died too early, in November 2004.

This work was supported by institutional funds from the Research and Education Ministries of France (PRFMMIP and Nanosciences ACI) and by a grant from the ARC (to M. Angelova).

REFERENCES

1. **Ahmed, S. N., D. A. Brown, and E. London.** 1997. On the origin of sphingolipid/cholesterol-rich detergent-insoluble cell membranes: physiological concentrations of cholesterol and sphingolipid induce formation of a detergent-insoluble, liquid-ordered lipid phase in model membranes. Biochemistry **36:**10944–10953.
2. **Anderson, R. G., and K. Jacobson.** 2002. A role for lipid shells in targeting proteins to caveolae, rafts, and other lipid domains. Science **296:**1821–1825.
3. **Bligh, E. G., and W. J. Dyer.** 1959. A rapid method of total lipid extraction and purification. Can. J. Biochem. Physiol. **37:**911–917.
4. **Boggs, J. M.** 1987. Lipid intermolecular hydrogen bonding: influence on structural organization and membrane function. Biochim. Biophys. Acta **906:**353–404.
5. **Böttcher, C., C. van Gent, and C. Pries.** 1961. A rapid and sensitive submicro phosphorus determination. Anal. Chim. Acta **24:**203–204.
6. **Braccia, A., M. Villani, L. Immerdal, L. L. Niels-Christiansen, B. T. Nystrom, G. H. Hansen, and E. M. Danielsen.** 2003. Microvillar membrane microdomains exist at physiological temperature. Role of galectin-4 as lipid raft stabilizer revealed by "superrafts." J. Biol. Chem. **278:**15679–15684.
7. **Breuza, L., S. Corby, J. P. Arsanto, M. H. Delgrossi, P. Scheiffele, and A. Le Bivic.** 2002. The scaffolding domain of caveolin 2 is responsible for its Golgi localization in Caco-2 cells. J. Cell Sci. **115:**4457–4467.
8. **Brown, D. A., and E. London.** 2000. Structure and function of sphingolipid- and cholesterol-rich membrane rafts. J. Biol. Chem. **275:**17221–17224.
9. **Brown, D. A., and E. London.** 1998. Structure and origin of ordered lipid domains in biological membranes. J. Membr. Biol. **164:**103–114.
10. **Brown, D. A., and J. K. Rose.** 1992. Sorting of GPI-anchored proteins to glycolipid-enriched membrane subdomains during transport to the apical cell surface. Cell **68:**533–544.
11. **Brown, R. E.** 1998. Sphingolipid organization in biomembranes: what physical studies of model membranes reveal. J. Cell Sci. **111:**1–9.
12. **Brugger, B., C. Graham, I. Leibrecht, E. Mombelli, A. Jen, F. Wieland, and R. Morris.** 2004. The membrane domains occupied by glycosylphosphatidylinositol-anchored prion protein and Thy-1 differ in lipid composition. J. Biol. Chem. **279:**7530–7536.
13. **Cane, A., M. Breton, G. Bereziat, and O. Colard.** 1997. Phospholipase A2-dependent and -independent pathways of arachidonate release from vascular smooth muscle cells. Biochem. Pharmacol. **53:**327–337.
14. **Chazal, N., and D. Gerlier.** 2003. Virus entry, assembly, budding, and membrane rafts. Microbiol. Mol. Biol. Rev. **67:**226–237.
15. **Ciarlet, M., and M. K. Estes.** 2001. Interactions between rotavirus and gastrointestinal cells. Curr. Opin. Microbiol. **4:**435–441.
16. **Cooper, D. N., and S. H. Barondes.** 1990. Evidence for export of a muscle lectin from cytosol to extracellular matrix and for a novel secretory mechanism. J. Cell Biol. **110:**1681–1691.
17. **Cuadras, M. A., B. B. Bordier, J. L. Zambrano, J. E. Ludert, and H. B. Greenberg.** 2006. Dissecting rotavirus particle-raft interaction with small interfering RNAs: insights into rotavirus transit through the secretory pathway. J. Virol. **80:**3935–3946.
18. **Cuadras, M. A., and H. B. Greenberg.** 2003. Rotavirus infectious particles use lipid rafts during replication for transport to the cell surface in vitro and in vivo. Virology **313:**308–321.
19. **de Almeida, R. F., A. Fedorov, and M. Prieto.** 2003. Sphingomyelin/phosphatidylcholine/cholesterol phase diagram: boundaries and composition of lipid rafts. Biophys. J. **85:**2406–2416.
20. **Delacour, D., V. Gouyer, J. P. Zanetta, H. Drobecq, E. Leteurtre, G. Grard, O. Moreau-Hannedouche, E. Maes, A. Pons, S. Andre, A. Le Bivic, H. J. Gabius, A. Manninen, K. Simons, and G. Huet.** 2005. Galectin-4 and sulfatides in apical membrane trafficking in enterocyte-like cells. J. Cell Biol. **169:**491–501.
21. **Delmas, O., A. M. Durand-Schneider, J. Cohen, O. Colard, and G. Trugnan.** 2004. Spike protein VP4 assembly with maturing rotavirus requires a pos-

tendoplasmic reticulum event in polarized Caco-2 cells. J. Virol. **78:**10987–10994.

22. **Delorme, C., H. Brussow, J. Sidoti, N. Roche, K. A. Karlsson, J. R. Neeser, and S. Teneberg.** 2001. Glycosphingolipid binding specificities of rotavirus: identification of a sialic acid-binding epitope. J. Virol. **75:**2276–2287.
23. **Denisova, E., W. Dowling, R. LaMonica, R. Shaw, S. Scarlata, F. Ruggeri, and E. R. Mackow.** 1999. Rotavirus capsid protein VP5* permeabilizes membranes. J. Virol. **73:**3147–3153.
24. **Dormitzer, P. R., Z. Y. Sun, G. Wagner, and S. C. Harrison.** 2002. The rhesus rotavirus VP4 sialic acid binding domain has a galectin fold with a novel carbohydrate binding site. EMBO J. **21:**885–897.
25. **Drevot, P., C. Langlet, X. J. Guo, A. M. Bernard, O. Colard, J. P. Chauvin, R. Lasserre, and H. T. He.** 2002. TCR signal initiation machinery is preassembled and activated in a subset of membrane rafts. EMBO J. **21:**1899–1908.
26. **Estes, M. K.** 2001. Rotaviruses and their replication, p. 1747–1785. *In* D. M. Knipe, P. M. Howley, D. E. Griffin, R. A. Lamb, M. A. Martin, B. Roizman, and S. E. Straus (ed.), Fields virology, 4th ed., vol. 2. Lippincott Williams & Wilkins, Philadelphia, PA.
27. **Foster, L. J., C. L. De Hoog, and M. Mann.** 2003. Unbiased quantitative proteomics of lipid rafts reveals high specificity for signaling factors. Proc. Natl. Acad. Sci. USA **100:**5813–5818.
28. **Gamble, W., M. Vaughan, H. S. Kruth, and J. Avigan.** 1978. Procedure for determination of free and total cholesterol in micro- or nanogram amounts suitable for studies with cultured cells. J. Lipid Res. **19:**1068–1070.
29. **Gardet, A., M. Breton, P. Fontanges, G. Trugnan, and S. Chwetzoff.** 2006. Rotavirus spike protein VP4 binds to and remodels actin bundles of the epithelial brush border into actin bodies. J. Virol. **80:**3947–3956.
30. **Golantsova, N. E., E. E. Gorbunova, and E. R. Mackow.** 2004. Discrete domains within the rotavirus VP5* direct peripheral membrane association and membrane permeability. J. Virol. **78:**2037–2044.
31. **Gomez-Mouton, C., J. L. Abad, E. Mira, R. A. Lacalle, E. Gallardo, S. Jimenez-Baranda, I. Illa, A. Bernad, S. Manes, and A. C. Martinez.** 2001. Segregation of leading-edge and uropod components into specific lipid rafts during T cell polarization. Proc. Natl. Acad. Sci. USA **98:**9642–9647.
32. **Graham, K. L., P. Halasz, Y. Tan, M. J. Hewish, Y. Takada, E. R. Mackow, M. K. Robinson, and B. S. Coulson.** 2003. Integrin-using rotaviruses bind $\alpha2\beta1$ integrin $\alpha2$ I domain via VP4 DGE sequence and recognize $\alpha X\beta2$ and $\alpha V\beta3$ by using VP7 during cell entry. J. Virol. **77:**9969–9978.
33. **Guerrero, C. A., S. Zarate, G. Corkidi, S. Lopez, and C. F. Arias.** 2000. Biochemical characterization of rotavirus receptors in MA104 cells. J. Virol. **74:**9362–9371.
34. **Hansen, G. H., L. Immerdal, E. Thorsen, L. L. Niels-Christiansen, B. T. Nystrom, E. J. Demant, and E. M. Danielsen.** 2001. Lipid rafts exist as stable cholesterol-independent microdomains in the brush border membrane of enterocytes. J. Biol. Chem. **276:**32338–32344.
35. **Ikonen, E.** 2001. Roles of lipid rafts in membrane transport. Curr. Opin. Cell Biol. **13:**470–477.
36. **Ilangumaran, S., and D. C. Hoessli.** 1998. Effects of cholesterol depletion by cyclodextrin on the sphingolipid microdomains of the plasma membrane. Biochem. J. **335:**433–440.
37. **Isa, P., M. Realpe, P. Romero, S. Lopez, and C. F. Arias.** 2004. Rotavirus RRV associates with lipid membrane microdomains during cell entry. Virology **322:**370–381.
38. **Iwabushi, K., K. Handa, and S. Hakomori.** 1998. Separation of "glycosphingolipid signaling domain" from caveolin-containing membrane fraction in mouse melanoma B16 cells and its role in cell adhesion coupled with signaling. J. Biol. Chem. **273:**33766–33773.
39. **Johnson, S. B., and R. E. Brown.** 1992. Simplified derivatization for determining sphingolipid fatty acyl composition by gas chromatography-mass spectrometry. J. Chromatogr. **605:**281–286.
40. **Jourdan, N., M. Maurice, D. Delautier, A. M. Quero, A. L. Servin, and G. Trugnan.** 1997. Rotavirus is released from the apical surface of cultured human intestinal cells through nonconventional vesicular transport that bypasses the Golgi apparatus. J. Virol. **71:**8268–8278.
41. **Keller, P., and K. Simons.** 1998. Cholesterol is required for surface transport of influenza virus hemagglutinin. J. Cell Biol. **140:**1357–1367.
42. **Mackow, E. R., R. D. Shaw, S. M. Matsui, P. T. Vo, M. N. Dang, and H. B. Greenberg.** 1988. The rhesus rotavirus gene encoding protein VP3: location of amino acids involved in homologous and heterologous rotavirus neutralization and identification of a putative fusion region. Proc. Natl. Acad. Sci. USA **85:**645–649.
43. **Madore, N., K. L. Smith, C. H. Graham, A. Jen, K. Brady, S. Hall, and R. Morris.** 1999. Functionally different GPI proteins are organized in different domains on the neuronal surface. EMBO J. **18:**6917–6926.
44. **Masserini, M., and D. Ravasi.** 2001. Role of sphingolipids in the biogenesis of membrane domains. Biochim. Biophys. Acta **1532:**149–161.
45. **Mirre, C., L. Monlauzeur, M. Garcia, M. H. Delgrossi, and A. Le Bivic.** 1996. Detergent-resistant membrane microdomains from Caco-2 cells do not contain caveolin. Am. J. Physiol. **271:**C887–C894.
46. **Musalem, C., and R. T. Espejo.** 1985. Release of progeny virus from cells infected with simian rotavirus SA11. J. Gen. Virol. **66:**2715–2724.
47. **Nandi, P., A. Charpilienne, and J. Cohen.** 1992. Interactions of rotavirus particles with liposomes. J. Virol. **66:**3363–3367.
48. **Nejmeddine, M., G. Trugnan, C. Sapin, E. Kholi, L. Svensson, S. Lopez, and J. Cohen.** 2000. Rotavirus spike protein VP4 is present at the plasma membrane and is associated with microtubules in infected cells. J. Virol. **74:**3313–3320.
49. **Nickel, W.** 2003. The mystery of nonclassical protein secretion. A current view on cargo proteins and potential export routes. Eur. J. Biochem. **270:**2109–2119.
50. **Ohvo, H., and J. P. Slotte.** 1996. Cyclodextrin-mediated removal of sterols from monolayers: effects of sterol structure and phospholipids on desorption rate. Biochemistry **35:**8018–8024.
51. **Pink, D. A., D. M. Chisholm, and D. Chapman.** 1988. Models of protein lateral arrangements in lipid bilayer membranes. Application to electron spin resonance studies of cytochrome c oxidase. Chem. Phys. Lipids **46:**267–277.
52. **Pralle, A., P. Keller, E. L. Florin, K. Simons, and J. K. Horber.** 2000. Sphingolipid-cholesterol rafts diffuse as small entities in the plasma membrane of mammalian cells. J. Cell Biol. **148:**997–1008.
53. **Ramstedt, B., and J. P. Slotte.** 1999. Interaction of cholesterol with sphingomyelins and acyl-chain-matched phosphatidylcholines: a comparative study of the effect of the chain length. Biophys. J. **76:**908–915.
54. **Röper, K., D. Corbeil, and W. B. Huttner.** 2000. Retention of prominin in microvilli reveals distinct cholesterol-based lipid microdomains in the apical plasma membrane. Nat. Cell Biol. **2:**582–592.
55. **Rouquette-Jazdanian, A. K., C. Pelassy, J. P. Breittmayer, and C. Aussel.** 2006. Revaluation of the role of cholesterol in stabilizing rafts implicated in T cell receptor signaling. Cell Signal. **18:**105–122.
56. **Sanchez-San Martin, C., T. Lopez, C. F. Arias, and S. Lopez.** 2004. Characterization of rotavirus cell entry. J. Virol. **78:**2310–2318.
57. **Sapin, C., O. Colard, O. Delmas, C. Tessier, M. Breton, V. Enouf, S. Chwetzoff, J. Ouanich, J. Cohen, C. Wolf, and G. Trugnan.** 2002. Rafts promote assembly and atypical targeting of a nonenveloped virus, rotavirus, in Caco-2 cells. J. Virol. **76:**4591–4602.
58. **Schuck, S., M. Honsho, K. Ekroos, A. Shevchenko, and K. Simons.** 2003. Resistance of cell membranes to different detergents. Proc. Natl. Acad. Sci. USA **100:**5795–5800.
59. **Sharma, P., R. Varma, R. C. Sarasij, Ira, K. Gousset, G. Krishnamoorthy, M. Rao, and S. Mayor.** 2004. Nanoscale organization of multiple GPI-anchored proteins in living cell membranes. Cell **116:**577–589.
60. **Simons, K., and E. Ikonen.** 1997. Functional rafts in cell membranes. Nature **387:**569–572.
61. **Simons, K., and D. Toomre.** 2000. Lipid rafts and signal transduction. Nat. Rev. Mol. Cell. Biol. **1:**31–39.
62. **Slimane, T. A., G. Trugnan, S. C. Van IJzendoom, and D. Hoekstra.** 2003. Raft-mediated trafficking of apical resident proteins occurs in both direct and transcytotic pathways in polarized hepatic cells: role of distinct lipid microdomains. Mol. Biol. Cell **14:**611–624.
63. **Stryer, L.** 1975. Biochemistry, biosynthesis of membrane lipids. W. H. Freeman, San Francisco, CA.
64. **van Meer, G., and J. C. Holthuis.** 2000. Sphingolipid transport in eukaryotic cells. Biochim. Biophys. Acta **1486:**145–170.
65. **Varma, R., and S. Mayor.** 1998. GPI-anchored proteins are organized in submicron domains at the cell surface. Nature **394:**798–801.
66. **Volonte, D., F. Galbiati, S. Li, K. Nishiyama, T. Okamoto, and M. P. Lisanti.** 1999. Flotillins/cavatellins are differentially expressed in cells and tissues and form a hetero-oligomeric complex with caveolins in vivo. Characterization and epitope-mapping of a novel flotillin-1 monoclonal antibody probe. J. Biol. Chem. **274:**12702–12709.